



This is an *Accepted Manuscript*, which has been through the RSC Publishing peer review process and has been accepted for publication.

*Accepted Manuscripts* are published online shortly after acceptance, which is prior to technical editing, formatting and proof reading. This free service from RSC Publishing allows authors to make their results available to the community, in citable form, before publication of the edited article. This *Accepted Manuscript* will be replaced by the edited and formatted *Advance Article* as soon as this is available.

To cite this manuscript please use its permanent Digital Object Identifier (DOI®), which is identical for all formats of publication.

More information about *Accepted Manuscripts* can be found in the [Information for Authors](#).

Please note that technical editing may introduce minor changes to the text and/or graphics contained in the manuscript submitted by the author(s) which may alter content, and that the standard [Terms & Conditions](#) and the [ethical guidelines](#) that apply to the journal are still applicable. In no event shall the RSC be held responsible for any errors or omissions in these *Accepted Manuscript* manuscripts or any consequences arising from the use of any information contained in them.

Cite this: DOI: 10.1039/c0xx00000x

www.rsc.org/xxxxxx

# A quinoxaline-fused tetrathiafulvalene derivative and its semiconducting charge-transfer salt: synthesis, crystal structures and physical properties

Yan Geng,<sup>a</sup> Christoph Fiolka,<sup>a</sup> Karl Krämer,<sup>a</sup> Jürg Hauser,<sup>a</sup> Vladimir Laukhin,<sup>b</sup> Silvio Decurtins<sup>a</sup> and Shi-Xia Liu<sup>\*a</sup>

Received (in XXX, XXX) Xth XXXXXXXXXX 20XX, Accepted Xth XXXXXXXXXX 20XX

DOI: 10.1039/b000000x

A quinoxaline-fused tetrathiafulvalene (TTF) derivative **1** has been synthesized to form a compact and planar  $\pi$ -conjugated donor-acceptor (D- $\pi$ -A) ensemble, and its single crystal structure has been determined by X-ray diffraction. The inherent redox activity of **1** has been probed by cyclic voltammetry, and UV-vis spectroscopy revealed the typical broad and intense intramolecular charge-transfer (ICT) absorption occurring for such compactly fused D- $\pi$ -A molecules. Reaction with iodine led to a 2:1 semiconducting charge-transfer salt  $\{(\mathbf{1})_2\text{I}_3\}$ , whose single crystal structure investigation, however, underlined the occurrence of a pronounced charge localization for the organic lattice. Consequently, the electrical conductivity of  $\{(\mathbf{1})_2\text{I}_3\}$ , measured with the four contacts method on single crystals, gave only a limited value of about  $1 \times 10^{-4} \Omega^{-1} \text{cm}^{-1}$ , and the activation energy was determined to be on the order of 470–480 meV.

## Introduction

Tetrathiafulvalene (TTF) and its derivatives are strong  $\pi$ -donors capable of forming, upon oxidation, persistent cation radical species leading to a wide variety of charge-transfer (CT) salts which include semiconductors, metals and superconductors.<sup>1-7</sup> Among these salts, those comprising a formally half-charged TTF unit (TTF<sup>0.5+</sup>) and 2D conducting and cationic donor sheets are usually the most conductive.<sup>1,2</sup> It has also been demonstrated that the packing arrangement of the donor molecules as well as the symmetry and size of the counterions strongly determine the transport properties of these salts. As a consequence, much effort has been devoted to the chemical modification of the donor atoms (S) of tetrathiafulvalene series<sup>8,9</sup> or the attachment of functional groups to the core of the donor frameworks<sup>10-20</sup> for an enhancement of the intermolecular interactions among electron donors and acceptors (or counter anions). The latter is essential to stabilize the conducting and superconducting states (suppressing the Peierls distortions) at low temperature. For instance, intriguing electronic effects of H-bond interactions can play an important role in the molecular arrangement and physical properties of the CT complexes.<sup>14-20</sup> In this context, a promising strategy for fine-tuning the electronic states, molecular arrangements, and solid-state physical properties of CT salts can be the direct annulation of  $\pi$ -electron acceptors to the TTF core.

In 2006, for the first time we developed an efficient synthetic approach to 5,6-diamino-2-(4,5-bis(propylthio)-1,3-dithio-2-ylidene)benzo[*d*]1,3-dithiole (Scheme 1).<sup>21</sup> With this key precursor in hand, the Schiff-base reaction has been successfully applied to prepare various TTF-fused donor-acceptor (D- $\pi$ -A) ensembles, which inherently show structurally rigid and planar

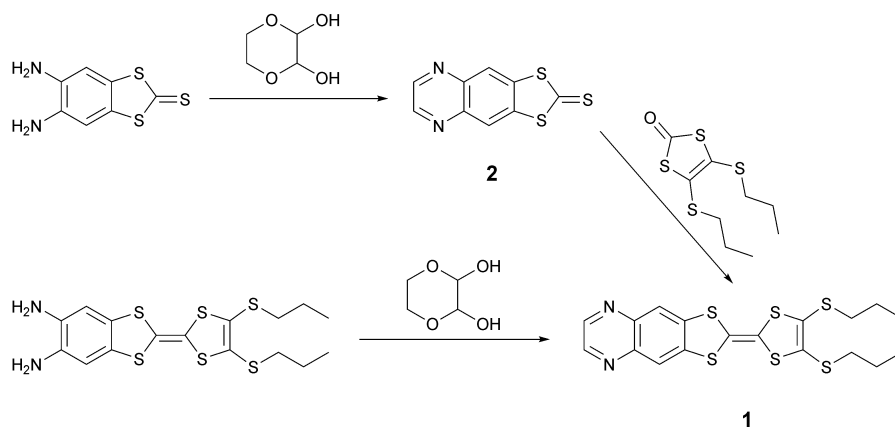
molecular conformations.<sup>21-28</sup> In contrast to D- $\sigma$ -A ensembles, sterically controlled and compactly fused D- $\pi$ -A systems exhibit pronounced photo-induced charge-transfer processes giving rise to interesting photophysical phenomena such as long-lived charge-separated states.<sup>29</sup> Moreover, such  $\pi$ -conjugated systems allow the combination of an energetically high-lying HOMO (highest occupied molecular orbital) localized on D with a low-lying LUMO (lowest unoccupied molecular orbital) localized on A, resulting in small HOMO-LUMO energy gaps,<sup>24</sup> which are of current interest in molecular (opto)electronics. With these considerations in mind, a quinoxaline-fused TTF derivative **1** comprising two redox active centers has been synthesized and structurally characterized. By cyclic voltammetry and optical spectroscopy measurements, the various redox states and the electronically excited states were determined. Notably, also a CT salt of formula  $\{(\mathbf{1})_2\text{I}_3\}$  has been obtained and structurally characterized; its electrical conductivity and magnetic susceptibility data are reported.

## Results and discussion

### Synthesis and crystal structures of **1** and $\{(\mathbf{1})_2\text{I}_3\}$

As illustrated in Scheme 1, the target compound **1** was obtained by a phosphite-mediated cross-coupling reaction of 4,5-bis(propylthio)-1,3-dithiole-2-one with the key precursor **2**, the synthesis of which was accomplished in 70% yield via direct condensation of 5,6-diaminobenzene-1,3-dithiole-2-thione with 1,4-dioxane-2,3-diol. Alternatively, the direct condensation reaction of 5,6-diamino-2-(4,5-bis(propylthio)-1,3-dithio-2-ylidene)benzo[*d*]1,3-dithiole with 1,4-dioxane-2,3-diol afforded **1** in 96% yield. By slow evaporation of a solution of **1** and iodine in

a mixture of CH<sub>3</sub>CN and CH<sub>2</sub>Cl<sub>2</sub>, black single crystals of the charge transfer salt  $\{(1)_2I_3\}$  were obtained.



Scheme 1 Synthetic routes to the target compound 1

Table 1 Data collection and refinement parameters for 1 and its charge transfer salt  $\{(1)_2I_3\}$

	1	$\{(1)_2I_3\}$
Formula	C <sub>18</sub> H <sub>18</sub> N <sub>2</sub> S <sub>6</sub>	C <sub>36</sub> H <sub>36</sub> I <sub>3</sub> N <sub>4</sub> S <sub>12</sub>
Formula weight	454.70	1290.11
Color	red	black
Crystal system	Triclinic	Triclinic
Space group	<i>P</i> -1	<i>P</i> -1
<i>a</i> [Å]	7.15364(18)	7.59591(8)
<i>b</i> [Å]	7.3059(2)	11.61481(13)
<i>c</i> [Å]	19.4670(5)	25.9543(3)
$\alpha$ [°]	91.284(2)	83.0995(10)
$\beta$ [°]	90.918(2)	84.6415(9)
$\gamma$ [°]	102.456(2)	89.8152(9)
<i>V</i> [Å <sup>3</sup> ]	992.99(5)	2263.22(4)
<i>Z</i>	2	2
$\rho_{\text{calc}}$ [g/cm <sup>3</sup> ]	1.521	1.893
$\mu$ [mm <sup>-1</sup> ]	0.695	2.659
<i>R</i> <sub>int</sub>	0.0229	0.044
No. Refl.	24762	161756
Independent reflections	4913	13791
Goodness-of-fit on <i>F</i> <sup>2</sup>	1.046	1.165
<i>R</i> <sub>1</sub> ; <i>wR</i> <sub>2</sub> [ <i>I</i> > 2 $\sigma$ ( <i>I</i> )]	0.0274; 0.0666	0.0297; 0.062
<i>R</i> <sub>1</sub> ; <i>wR</i> <sub>2</sub> (all data)	0.0331; 0.0702	0.0362; 0.0661
$\Delta\rho_{\text{max}}$ ; $\Delta\rho_{\text{min}}$ [e Å <sup>-3</sup> ]	0.332; -0.252	1.516; -1.31

Compound 1 crystallises in a solvate free form in the triclinic space group *P*-1 (Table 1) and the red colored crystals have a plate-shaped morphology. The asymmetric unit comprises one complete molecule, thus all atoms lie on general positions. An ORTEP drawing is shown in Fig. 1a. A large part of the  $\pi$ -conjugated skeleton is virtually planar and only along the S3–S4 “axis” occurs a slight bending which is, however, typical for neutral TTF units. Fig. 1b highlights the mutual arrangement of the molecules in the crystal structure. A noticeable feature is the parallel head-to-tail alignment of dimers which stack along the *a* axis with some close contacts of 3.300 (C1···C5) and 3.330 (C2···C4) Å. The shortest interdimer contact is 3.462 (C4···S2) Å.

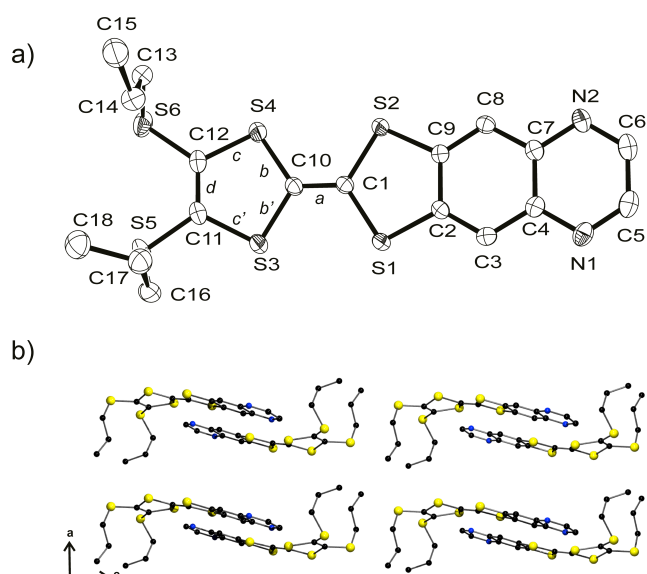
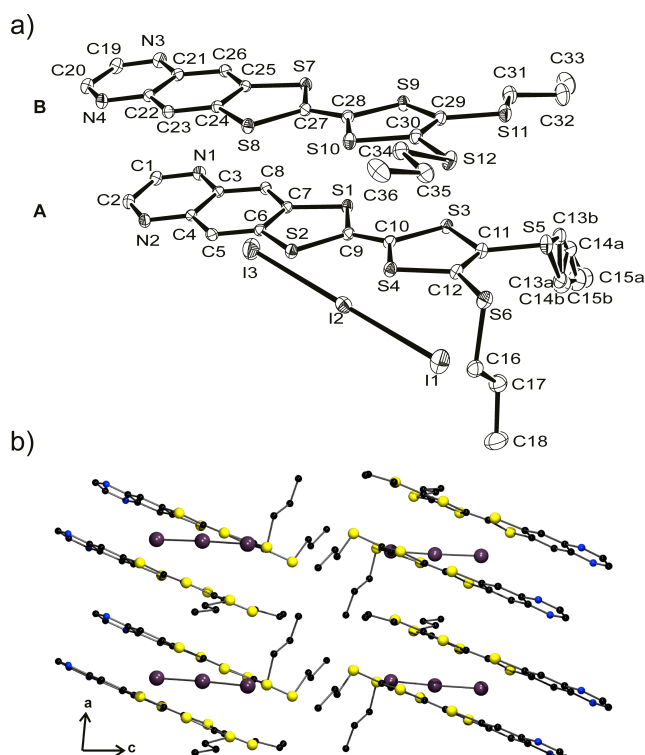


Fig. 1 (a) ORTEP view of molecule 1 (the thermal ellipsoids are shown at the 50% probability level); hydrogen atoms have been omitted for clarity. (b) Projection of the crystal structure on the *ac* plane.

The charge transfer salt  $\{(1)_2I_3\}$  crystallises in a solvate free form in the triclinic space group *P*-1 (Table 1) and the black crystals exhibit an elongated plate-shaped morphology. The asymmetric unit comprises two crystallographically independent molecules 1A and 1B which bear in total one positive charge and one triiodide anion. An ORTEP drawing is shown in Fig. 2a. In contrast to the neutral compound 1, there is a parallel head-to-head arrangement of adjacent molecules leading to stacks with an  $\cdots 1A \cdots 1B \cdots 1A \cdots 1B \cdots$  arrangement along the *a* axis (Fig. 2b). The crystal structure reveals close C···S contacts of 3.486 (C6···S8), 3.492 (C29···S3) and 3.436 (C23···S8) Å, as well as a S4···S10 contact of 3.585 Å. Intermolecular CH···N hydrogen bonds of 3.224 (C19···N1) and 3.243 (C1···N3) Å link the donor stacks along the *b* direction. However, triiodide anions separate the donor units along the *b* direction and also no short S···S contacts occur along the *b* axis.

The molecular  $\pi$ -conjugated skeletons of 1A and 1B in the CT

salt are planar; the rms deviation from a least-squares plane through all atoms, excluding the two peripheral propyl groups, is 0.063 Å (**1A**) and 0.050 Å (**1B**), respectively. Similarly, a least-squares plane through the atoms of the TTF cores alone reveals a rms deviation of only 0.036 Å (**1A**) and 0.041 Å (**1B**), respectively.



**Fig. 2** (a) ORTEP view of the charge transfer salt  $\{(1)_2I_3\}$  (the thermal ellipsoids are shown at the 30% probability level); hydrogen atoms have been omitted for clarity. (b) Representation of the crystal structure with a view on the  $ac$  plane.

Moreover, the two crystallographically independent and partially charged molecules **1A** and **1B** possess distinctly different structural parameters, as e.g. confirmed by differences in the C=C double bond length and the C–S distances of the dithiole rings (labelled as  $a\dots d$  in Fig. 1a, Table 2). These distances depend most sensitively on the oxidation state or degree of partial charge of the TTF moiety in the molecule. For instance for TTF, the average bond length of the central C=C bond is 1.32 Å in the neutral state and 1.38 Å in the fully oxidised monocationic state.<sup>30</sup> Thus, it can be inferred that in the salt  $\{(1)_2I_3\}$  the molecule **1B** exhibits approximately a fully charged state and consequently molecule **1A** remains essentially in the neutral state. As a result, the single crystals show a relatively high electrical resistance (see below).

**Table 2** Selected bond lengths (Å)<sup>a</sup> of **1** and  $\{(1)_2I_3\}$

	<b>1</b>	$\{(1)_2I_3\}$	
		Molecule <b>1A</b>	Molecule <b>1B</b>
<i>a</i>	1.3446 (19)	1.353 (3)	1.380 (3)
<i>b</i>	1.757 (2)	1.755 (3)	1.725 (3)
<i>c</i>	1.763 (2)	1.751 (3)	1.735 (3)
<i>d</i>	1.347 (2)	1.351 (3)	1.372 (3)

<sup>a</sup> Labels  $a\dots d$  refer to Fig. 1; average values are used for *b* and *c*.

### 30 Redox and photophysical properties of **1**

The electrochemical properties of **1** in  $CH_2Cl_2$  were investigated by cyclic voltammetry. In analogy to the previously reported TTF-dppz<sup>22</sup> (dppz = dipyridophenazine), **1** can be oxidized to its radical cation (**1<sup>•+</sup>**) and dication (**1<sup>2+</sup>**) sequentially and reversibly at  $E_{1/2}^{ox1} = 0.71$  V and  $E_{1/2}^{ox2} = 1.08$  V vs Ag/AgCl, respectively. Moreover, **1** exhibits one reversible reduction wave at  $E_{1/2}^{red} = -1.52$  V vs Ag/AgCl, corresponding to the reduction of the quinoxaline moiety.

The optical absorption spectrum of **1** in THF solution is shown in Fig. 3. In analogy to a similarly fused quinoxaline-TTF compound,<sup>31</sup> the intense absorption bands at 250 nm and 330 nm are assigned to  $\pi\pi^*$  transitions which are mainly localised on the quinoxaline and TTF moieties. The absorption pattern in the visible spectral region is dominated by a broad and intense band centered at 458 nm with a molar extinction coefficient of  $10^4$  M<sup>-1</sup> cm<sup>-1</sup>. This electronic excitation is typical for fused D- $\pi$ -A molecules,<sup>22</sup> and essentially it corresponds to an intramolecular charge-transfer transition (ICT), being a one-electron excitation from the HOMO localized on the TTF moiety to the LUMO localized on quinoxaline fragment. Moreover, **1** shows a weak fluorescence from its CT state, peaking at 656 nm with a quantum yield of 0.6%. The fluorescence excitation spectrum, measured at 620 nm emission wavelength, agrees well with the corresponding absorption profile. Taking the crossing-point of the absorption and emission spectra (557 nm), an optical HOMO–LUMO gap of 2.23 eV is calculated which matches perfectly with the electrochemical HOMO–LUMO gap of 2.23 eV ( $E_{gap} = E_{1/2}^{ox1} - E_{1/2}^{red}$ ).

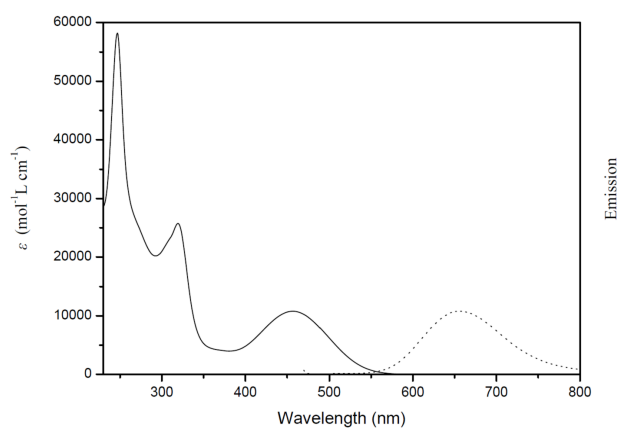


**Fig. 3** Absorption and emission spectra ( $\lambda_{ex} = 460$  nm) of **1** in THF solution at room temperature.

### Electrical conductivity and magnetic susceptibility of $\{(1)_2I_3\}$

The electrical resistance for several single crystals of the CT salt  $\{(1)_2I_3\}$  was measured with the four contacts method, and their room temperature values were all relatively high, namely  $> 10^6$  Ω, but they decrease with increasing temperatures (Fig. 4). This rather high resistance results in a limited conductivity of the order of  $1 \times 10^{-4}$  Ω<sup>-1</sup> cm<sup>-1</sup>. In order to estimate the activation energy (at least around room temperature) the samples were heated up to 348 K and the  $\ln R$  vs  $1/T$  relation gives values in the range of

470 – 480 meV.

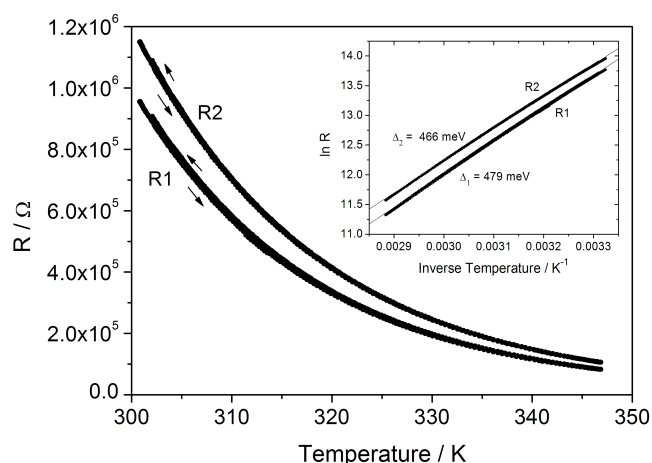


Fig. 4 Plot of electrical resistance vs temperature for two crystals of  $\{(1)_2I_3\}$ . Inset: the Arrhenius plot of electrical resistivity as a function of the reciprocal temperature.

The magnetic susceptibility data of a polycrystalline sample of  $\{(1)_2I_3\}$  are displayed in Fig. 5 as  $\chi_m T$  vs  $T$  plot. According to the equation,  $\chi_m T = \chi_{TIP} T + C$ , one can deduce that the magnetic behaviour is dominated by a temperature independent paramagnetism ( $TIP = 2.6 \times 10^{-3} \text{ emu mol}^{-1}$ ) originating from the Pauli paramagnetism of the organic lattice. There is also an additional and substantial paramagnetic contribution ( $C = 0.13 \text{ emu K mol}^{-1}$ ). Notably, the  $\chi_m T$  vs  $T$  behaviour as well as the TIP and  $C$  values correspond quite closely to a semiconducting bis(ethylendithio)tetrathiafulvalene (ET) type of CT compound.<sup>32</sup> The latter compound comprises three different types of ET molecules, whereby two of them are almost completely oxidized and one appears to be almost neutral. It turns out that the actual compound with an analogous charge localization on the organic lattice exhibits a quite similar magnetic behaviour.

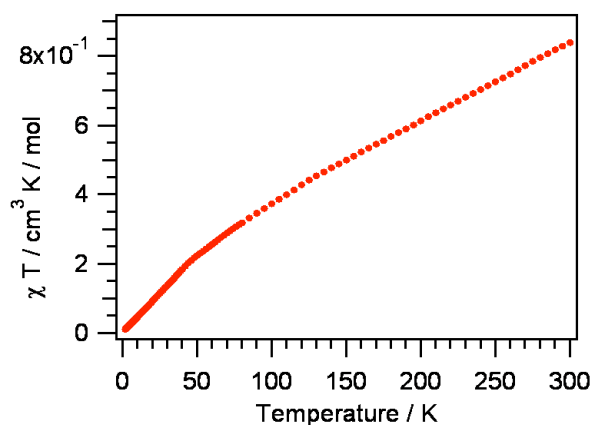


Fig. 5 Magnetic susceptibility of  $\{(1)_2I_3\}$  as  $\chi_m T$  vs  $T$  plot.

## Conclusion

We have synthesised a compact new donor-acceptor (D- $\pi$ -A) type molecule **1** while annulating the  $\pi$ -electron donor tetrathiafulvalene to the  $\pi$ -electron acceptor quinoxaline. Consequently, the planar  $\pi$ -conjugated molecule possesses two

redox active sites and shows an intense, broad and energetically low-lying charge-transfer absorption in the visible spectral region, which is quite remarkable for a small  $\pi$ -conjugated molecule. A semiconducting charge-transfer salt of formula  $\{(1)_2I_3\}$  resulted from a reaction of **1** with iodine. Due to a pronounced charge localization on the organic lattice, the single crystals show only a limited electrical conductivity.

## Experimental

### Materials and measurements

Air- and/or water-sensitive reactions were conducted under nitrogen using dry, freshly distilled solvents. Unless otherwise stated, all reagents were purchased from commercial sources and used without additional purification. The precursors, 1,4-dioxane-2,3-diol,<sup>33</sup> 4,5-bis(propylthio)-1,3-dithiole-2-one,<sup>34,35</sup> 5,6-diaminobenzene-1,3-dithiole-2-thione<sup>21,22</sup> and 5,6-diamino-2-(4,5-bis(propylthio)-1,3-dithio-2-ylidene)benzo[*d*][1,3]dithiole<sup>21,22</sup> were prepared according to the literature procedures. Elemental analysis was performed on a Carlo Erba Instruments EA 1110 Elemental Analyzer CHN. Infrared spectra were recorded on a Perkin-Elmer Spectrum One FT-IR spectrometer using KBr pellets. <sup>1</sup>H and <sup>13</sup>C NMR spectra were recorded at 300 and 75 MHz, respectively. Chemical shift in ppm is quoted relative to residual solvent signals calibrated as follows: CDCl<sub>3</sub>  $\delta_H$  (CHCl<sub>3</sub>) = 7.26 ppm,  $\delta_C$  = 77.0 ppm. Multiplicities in the <sup>1</sup>H NMR spectrum are described as: s = singlet, d = doublet, t = triplet, m = multiplet; coupling constants are reported in Hz. High-resolution mass spectrum was recorded with ESI (electrospray ionization) on a Thermo Scientific LTQ Orbitrap XL in the positive mode. Optical absorption spectra were recorded on a Cary 5000 UV/vis spectrophotometer. Emission and excitation spectra were measured on a Horiba Fluorolog 3. The luminescence quantum yield  $\Phi_F$  of **1** was determined by relative measurements<sup>36</sup> with respect to the standard value of a solution of Rhodamin 6G in EtOH ( $\Phi_F = 95\%$ ) at the excitation wavelength 480 nm.<sup>37</sup>

Cyclic voltammetry was conducted on a PGSTAT 101 potentiostat. An Ag/AgCl electrode containing 2 M LiCl (in ethanol) served as reference electrode, a glassy carbon electrode as counter electrode, and a Pt-disk as working electrode. Cyclic voltammetric measurements were performed at room temperature under Ar in CH<sub>2</sub>Cl<sub>2</sub> ( $1 \times 10^{-4}$  M) with 0.1 M *n*-Bu<sub>4</sub>NPF<sub>6</sub> as supporting electrolyte at a scan rate of 100 mV/s.

The powder X-ray diffraction pattern was recorded on a STOE spellmann generator type DF4 with a Cu anode.

Electrical resistivity measurements of  $\{(1)_2I_3\}$  were performed on several single crystals using a standard four-probe dc-method. Four annealed platinum wires (20  $\mu\text{m}$  in diameter) were attached to the crystals by a conductive graphite paste. All four contacts were placed on the same elongated surface of the crystals.

Magnetic susceptibility data of  $\{(1)_2I_3\}$  were recorded using a Quantum design MPMS-5XL SQUID magnetometer as a function of temperature (1.9–300 K) at a magnetic field of 0.5 T. Experimental data were corrected for sample holder and diamagnetic contributions calculated from  $-0.45 \times \text{molecular weight} \times 10^{-6} \text{ cm}^3 \text{ mol}^{-1}$ . The polycrystalline sample, whose crystalline phase was checked by its powder X-ray diffraction



pattern to be identical to the single crystal structure was pressed into a pellet to obtain a uniform shape.

### Syntheses

**Preparation of [1,3]dithiolo[4,5-g]quinoxalin-2-thione (2).** Acetic acid (20 mL) was added to a solution of 5,6-diaminobenzene-1,3-dithiole-2-thione (428 mg, 2 mmol) and 1,4-dioxane-2,3-diol (288 mg, 2.4 mmol) in EtOH (30 mL) under Ar. The mixture was refluxed for 16 h. After cooling to room temperature and filtration, the crude product was collected and purified by column chromatography on neutral Al<sub>2</sub>O<sub>3</sub> using dichloromethane as eluent to afford **2** (330 mg, 70%) as a light yellow solid. m.p. >270 °C (dec.); <sup>1</sup>H NMR (300 MHz, CDCl<sub>3</sub>) δ (ppm): 8.87 (s), 8.19 (s); <sup>13</sup>C NMR (300 MHz, CDCl<sub>3</sub>) δ (ppm): 211.7, 145.8, 143.9, 141.4, 121.2; IR data (KBr pellet) ν (cm<sup>-1</sup>): 3436, 2960, 1635, 1454, 1355, 1337, 1179, 1079, 1013, 930, 894, 886, 602; Elemental analysis of C<sub>9</sub>H<sub>4</sub>N<sub>2</sub>S<sub>3</sub>: calcd C 45.74, H 1.71, N 11.85%; found: C 45.80, H 1.76, N 11.69%.

**Preparation of 2-[4,5-bis(propylsulfanyl)-1,3-dithiol-2-ylidene][1,3]dithiolo[4,5-g]quinoxaline (1). Method 1:** Triethyl phosphite (6 mL) was added to a solution of **2** (236 mg, 1 mmol) and 4,5-bis(propylthio)-1,3-dithiole-2-one (532 mg, 2 mmol) in toluene (10 mL) under Ar. The mixture was refluxed for 3 h. After cooling to room temperature and removal of toluene, the resulting mixture was poured on a silica gel column, initially using hexane as eluent to remove unreacted triethyl phosphite and then dichloromethane/THF = 1:1 to afford **1** (220 mg, 43%) as an orange solid. **Method 2:** To a suspension of 5,6-diamino-2-(4,5-bis(propylthio)-1,3-dithio-2-ylidene)benzo[*d*]1,3-dithiole (40 mg, 92.4 μmol) in ethanol (30 mL) and glacial acetic acid (3 mL) under reflux was added 1,4-dioxane-2,3-diol (14.4 mg, 120 μmol). The mixture was stirred overnight. After evaporation of the solvent, the crude product as a reddish oil was purified by chromatography on silica gel using dichloromethane/hexane (1/2, v/v) as eluent to afford the analytically pure **1** (40 mg, 96%) as an orange solid. M.p. 140-142°C; <sup>1</sup>H NMR (300 MHz, CDCl<sub>3</sub>) δ (ppm): 8.69 (s, 2H), 7.88 (s, 2H), 2.80-2.85 (t, *J* = 7.30 Hz, 4H), 1.58-1.79 (m, 4H), 1.00-1.05 (t, *J* = 7.30 Hz, 6H); <sup>13</sup>C NMR (300 MHz, CDCl<sub>3</sub>) δ (ppm): 144.7, 142.1, 127.9, 120.5, 115.7, 108.4, 38.5, 23.3, 13.3; IR data (KBr pellet) ν (cm<sup>-1</sup>): 3435, 2964, 2922, 2869, 1632, 1452, 1419, 1374, 1351, 1334, 1293, 1237, 1170, 1094, 1022, 963, 925, 885, 869, 776, 731, 679; HRMS (ESI): calcd for C<sub>18</sub>H<sub>18</sub>N<sub>2</sub>S<sub>6</sub> *m/z* = 453.9794, found 453.9783; Elemental analysis of C<sub>18</sub>H<sub>18</sub>N<sub>2</sub>S<sub>6</sub>: calcd C 47.54, H 3.99, N 6.16%; found C 47.15, H 3.82, N 6.01%. Single crystals suitable for X-ray analysis were obtained by slow evaporation of a dichloromethane/methanol (1/1) solution of **1**.

**Preparation of the charge-transfer salt {(1)<sub>2</sub>I<sub>3</sub>}. In a typical experiment, a solution of I<sub>2</sub> (0.02 mmol) in CH<sub>3</sub>CN (5 mL) was mixed with a solution of **1** (0.01 mmol) in dichloromethane (5 mL). The mixture was kept in the dark and black single crystals (18 mg, 27.9%) were formed after two weeks. M.p. 170-172°C; IR data (KBr pellet) ν (cm<sup>-1</sup>): 3436, 2965, 2922, 1633, 1453, 1229, 1146, 1098, 885; Elemental analysis of C<sub>36</sub>H<sub>36</sub>I<sub>3</sub>N<sub>4</sub>S<sub>12</sub>: calcd C 33.51, H 2.81, N 4.34%; found C 33.50, H 2.80, N 4.20%.**

### Crystal structure determination

Crystal structures were measured on a Oxford Diffraction SuperNova area-detector diffractometer using mirror optics monochromated Mo K<sub>α</sub> radiation (λ = 0.71073 Å) at 173 K. Data reduction was performed using the CrysAlisPro<sup>38</sup> program. The intensities were corrected for Lorentz and polarization effects and

a numerical absorption correction based on gaussian integration over a multifaceted crystal model using CrysAlisPro<sup>38</sup> for **1**, or an absorption correction based on the multi-scan method using SCALE3 ABSPACK in CrysAlisPro<sup>38</sup> for {(1)<sub>2</sub>I<sub>3</sub>} were applied. Data collection and refinement parameters are given in Table 1. The structures were solved by direct methods using SIR97,<sup>39</sup> which revealed the positions of all not disordered non-hydrogen atoms. The non-hydrogen atoms were refined anisotropically. All H-atoms were placed in geometrically calculated positions and refined using a riding model where each H-atom was assigned a fixed isotropic displacement parameter with a value equal to 1.2 U<sub>eq</sub> of its parent atom (1.5 U<sub>eq</sub> for methyl). In the case of {(1)<sub>2</sub>I<sub>3</sub>}, the geometries of the two sites of the disordered propyl group were restrained to be similar (SHELXL SAME instruction). Its adp's were restrained with SHELXL DELU, SIMU instructions. Refinement of the structure was carried out on F<sup>2</sup> using full-matrix least-squares procedures, which minimized the function Σw(F<sub>o</sub><sup>2</sup> - F<sub>c</sub><sup>2</sup>)<sup>2</sup>. The weighting scheme was based on counting statistics and included a factor to downweight the intense reflections. All calculations were performed using the SHELXL-97<sup>40</sup> program. CCDC reference numbers: **1** - 958950, {(1)<sub>2</sub>I<sub>3</sub>} - 958951.

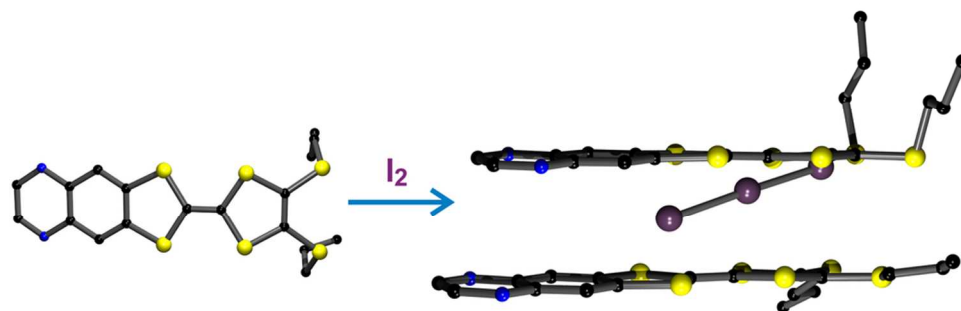
### Acknowledgements

Financial support for this research by the Swiss National Science Foundation (Grant No. 200021-147143) is gratefully acknowledged.

### Notes and references

- <sup>a</sup> *Departement für Chemie und Biochemie, Universität Bern, Freiestrasse 3, CH-3012 Bern, Switzerland. Fax: 41 31 6313995; Tel: 41 31 6314296; E-mail: liu@iac.unibe.ch*
- <sup>b</sup> *Institució Catalana de Recerca i Estudis Avançats (ICREA), 08010 Barcelona, Catalonia, Spain and Institut de Ciència de Materials de Barcelona (ICMAB-CSIC), Campus de la UAB, Bellaterra 08193, Catalonia, Spain.*
- J. Yamada and T. Sugimoto, *TFE Chemistry. Fundamentals and applications of Tetrathiafulvalene*; Springer Verlag, Berlin, 2004.
- J. M. Williams, J. R. Ferraro, R. J. Thorn, K. D. Carlson, U. Geiser, H. H. Wang, A. M. Kini and M.-H. Whangbo, *Organic Superconductors (including Fullerenes)*, Prentice Hall: Englewood Cliffs, 1992.
- T. Enoki and A. Miyazaki, *Chem. Rev.*, 2004, **104**, 5449.
- J. L. Segura and N. Martín, *Angew. Chem. Int. Ed.*, 2001, **40**, 1372.
- D. Canevet, M. Sallé, G. Zhang, D. Zhang and D. Zhu, *Chem. Commun.*, 2009, 2245.
- D. Lorcy, N. Bellec, M. Fourmigué and N. Avarvari, *Coord. Chem. Rev.*, 2009, **253**, 1398.
- J. Sun, X. Lu, J. Shao, X. Li, S. Zhang, B. Wang, J. Zhao, Y. Shao, R. Fang, Z. Wang, W. Yu and X. Shao, *Chem. Eur. J.*, 2013, **19**, 12517.
- D. Jérôme, A. Mazaud, M. Ribault and K. Bechgaard, *J. Phys. Lett.*, 1980, **41**, 95.
- D. Jérôme, *Science*, 1991, **252**, 1509.
- S.-X. Liu, S. Dolder, M. Pilkington and S. Decurtins, *J. Org. Chem.*, 2002, **67**, 3160.
- B. Domezq, T. Devic, M. Fourmigué, P. Auban-Senzier and E. Canadell, *J. Mater. Chem.*, 2001, **11**, 1570.
- N. Terkia-Derdra, R. Andreu, M. Sallé, E. Levillain, J. Orduna, J. Garín, E. Ortí, R. Viruela, R. Pou-Amérgo, B. Sahraoui, A. Gorgues, J.-F. Favard and A. Riou, *Chem. Eur. J.*, 2000, **6**, 1199.

- 13 C. Jia, S.-X. Liu, C. Ambrus, G. Labat, A. Neels and S. Decurtins, *Polyhedron*, 2006, **25**, 1613.
- 14 H. Kamo, A. Ueda, T. Isono, K. Takahashi and H. Mori, *Tetrahedron Lett.*, 2012, **53**, 4385.
- 15 T. Murata, K. Nakasuji and Y. Morita, *Eur. J. Org. Chem.*, 2012, 4123.
- 16 S.-X. Liu, A. Neels, H. Stoeckli-Evans, M. Pilkington, J. D. Wallis and S. Decurtins, *Polyhedron*, 2004, **23**, 1185.
- 17 S. C. Lee, A. Ueda, H. Kamo, K. Takahashi, M. Uruichi, K. Yamamoto, K. Yakushi, A. Nakao, R. Kumai, K. Kobayashi, H. Nakao, Y. Murakami and H. Mori, *Chem. Commun.*, 2012, **48**, 8673.
- 18 T. Murata, Y. Morita, K. Fukui, K. Sato, D. Shiomi, T. Takui, M. Maesato, H. Yakushi, G. Saito and K. Nakasuji, *Angew. Chem., Int. Ed.*, 2004, **43**, 6343.
- 19 M. Fourmigué and P. Batail, *Chem. Rev.*, 2004, **104**, 5379.
- 20 T. Murata, Y. Morita, Y. Yakiyama, K. Fukui, H. Yamochi, G. Saito and K. Nakasuji, *J. Am. Chem. Soc.*, 2007, **129**, 10837.
- 21 C.-Y. Jia, S.-X. Liu, C. Tanner, C. Leiggenger, L. Sanguinet, E. Levillain, S. Leutwyler, A. Hauser and S. Decurtins, *Chem. Commun.*, 2006, 1878.
- 22 C.-Y. Jia, S.-X. Liu, C. Tanner, C. Leiggenger, A. Neels, L. Sanguinet, E. Levillain, S. Leutwyler, A. Hauser and S. Decurtins, *Chem. Eur. J.*, 2007, **13**, 3804.
- 23 H.-P. Jia, S.-X. Liu, L. Sanguinet, E. Levillain and S. Decurtins, *J. Org. Chem.*, 2009, **74**, 5727.
- 24 X. Guégano, A. L. Kanibolotsky, C. Blum, S. F. Mertens, S.-X. Liu, A. Neels, H. Hagemann, P. J. Skabara, S. Leutwyler, T. Wandlowski, A. Hauser and S. Decurtins, *Chem. Eur. J.*, 2009, **15**, 63.
- 25 C. Goze, N. Dupont, E. Beitler, C. Leiggenger, H.-P. Jia, P. Monbaron, S.-X. Liu, A. Neels, A. Hauser and S. Decurtins, *Inorg. Chem.*, 2008, **47**, 11010.
- 26 M. Jaggi, C. Blum, N. Dupont, J. Grilj, S.-X. Liu, J. Hauser, A. Hauser and S. Decurtins, *Org. Lett.*, 2009, **11**, 3096.
- 27 M. Jaggi, C. Blum, B. S. Marti, S.-X. Liu, S. Leutwyler, S. Decurtins, *Org. Lett.*, 2010, **12**, 1344.
- 28 R. Pfattner, E. Pavlica, M. Jaggi, S.-X. Liu, S. Decurtins, G. Bratina, J. Veciana, M. Mas-Torrent and C. Rovira, *J. Mater. Chem. C*, 2013, **1**, 3985.
- 29 C. Goze, C. Leiggenger, S.-X. Liu, L. Sanguinet, E. Levillain, A. Hauser and S. Decurtins, *ChemPhysChem* 2007, **8**, 1504.
- 30 M. A. Beno, U. Geiser, A. M. Kini, H.-H. Wang, K. D. Carlson, M. M. Miller, T. J. Allen, J. A. Schlueter, R. B. Proksch and J. M. Williams, *Synth. Met.*, 1988, **27**, A209.
- 31 H.-P. Jia, J. Ding, Y.-F. Ran, S.-X. Liu, C. Blum, I. Petkova, A. Hauser and S. Decurtins, *Chem. Asian J.*, 2011, **6**, 3312.
- 32 E. Coronado, J. R. Galan-Mascaros, C. J. Gomez-Garcia, A. Murcia-Martinez and E. Canadell, *Inorg. Chem.*, 2004, **43**, 8072.
- 33 M. C. Venuti, *Synthesis*, 1982, 61.
- 34 J. A. Hansen, J. Becher, J. O. Jeppesen, E. Levillain, M. B. Nielsen, B. M. Petersen, J. C. Petersen and Y. Sahin, *J. Mater. Chem.*, 2004, **14**, 179.
- 35 N. Svenstrup, K. M. Rasmussen, T. Kruse Hansen and J. Becher, *Synthesis*, 1994, 809.
- 36 J. N. Demas and G. A. Crosby, *J. Phys. Chem.*, 1971, **75**, 991.
- 37 D. Magde, R. Wong and P. G. Seybold, *Photochem. Photobiol.* 2002, **75**, 327.
- 38 *Oxford Diffraction, CrysAlisPro (Version 1.171.34.36)*, Oxford Diffraction Ltd., Yarnton, Oxfordshire, UK, 2010.
- 39 A. Altomare, M. C. Burla, M. Camalli, G. Casciarano, C. Giacovazzo, A. Guagliardi, A. G. G. Moliterni, G. Polidori and R. Spagna, *J. Appl. Crystallogr.*, 1999, **32**, 115.
- 40 G. M. Sheldrick, *Acta Cryst. A64*, 2008, 112.



92x29mm (300 x 300 DPI)